Supporting Information

Carrier Concentration Dependent Conduction in Insulator-Doped Donor/Acceptor Chain Compounds

Masaki Nishio,[†] Norihisa Hoshino,[‡] Wataru Kosaka,[§] Tomoyuki Akutagawa,[‡] Hitoshi Miyasaka*[,§]

[†] Department of Chemistry, Division of Material Sciences, Graduate School of Natural Science and Technology, Kanazawa University, Kakuma-machi, Kanazawa 920-1192, Japan

[‡] Institute of Multidisciplinary Research for Advanced Materials, Tohoku University, 2-1-1 Katahira, Aoba-ku, Sendai 980-8577, Japan

[§] Institute for Materials Research, Tohoku University, 2-1-1 Katahira, Aoba-ku, Sendai 980-8577, Japan

E-mail: miyasaka@imr.tohoku.ac.jp

Experimental Section

Syntheses

All synthetic procedures were performed under a N_2 atmosphere using standard Schlenk techniques and a commercial glovebox. All chemicals were purchased as reagent grade from commercial sources. Solvents used were distilled under a N_2 atmosphere using common drying agents. The starting materials, $[Ru_2(2\text{-MeO-4-ClPhCO}_2)_4(THF)_2]$ and $[Rh_2(2\text{-MeO-4-ClPhCO}_2)_4(THF)_2]$, were synthesized in a similar manner reported previously.[1,2]

$[Ru_2(2\text{-MeO-4-ClPhCO}_2)_4(BTDA\text{-}TCNQ)]\cdot2.5(benzene)$ (1). An anisole solution (20 ml) of $[Ru_2(2\text{-MeO-4-ClPhCO}_2)_4(THF)_2]$ (54.5 mg, 0.05 mmol) was separated into 2 ml portions and placed in narrow diameter sealed glass tubes (ϕ: 8 mm) (bottom layer). A benzene solution (20 ml) of BTDA-TCNQ (16.0 mg, 0.05 mmol) was carefully placed in 2 ml portions on the bottom layer. After the glass tubes were turned upside down two times, the glass tubes were left undisturbed for one week or more to yield plate-shape brown crystals of **1**. Yields; 40.0 mg (55%). Elemental analysis (%) calcd for $[Ru_2(2\text{-MeO-4-ClPhCO}_2)_4(BTDA\text{-}TCNQ)]\cdot2.5(benzene)$ $C_{59}H_{39}Cl_4N_8O_{12}Ru_2S_2$: C, 48.53; H, 2.69; N, 7.66. Found: C, 48.67; H, 3.01; N, 7.47. FT-IR (KBr): $\nu(C\equiv N)$, 2189, 2171; $\nu(C=O)$, 1596, 1406, 1381.

$[Rh_2(2\text{-MeO-4-ClPhCO}_2)_4(BTDA\text{-}TCNQ)]\cdot2.5(benzene)$ (1-Rh). This compound was synthesized in a similar way to **1**, except $[Rh_2(2\text{-MeO-4-ClPhCO}_2)_4(THF)_2]$ (54.6 mg, 0.05 mmol) was used instead of $[Ru_2(2\text{-MeO-4-ClPhCO}_2)_4(THF)_2]$. Yields; 21.0 mg (29%). Elemental analysis (%) calcd for $[Rh_2(2\text{-MeO-4-ClPhCO}_2)_4(BTDA\text{-}TCNQ)]\cdot2.5(benzene)$ $C_{59}H_{39}Cl_4N_8O_{12}Rh_2S_2$: C, 48.41; H, 2.69; N, 7.66. Found: C, 48.67; H, 3.01; N, 7.47. FT-IR (KBr): $\nu(C\equiv N)$, 2233, 2219; $\nu(C=O)$, 1602, 1407, 1377.

Rh-doped samples. The Rh-doped samples were synthesized in a similar way to **1** except mixture of $[Ru_2(2\text{-MeO-4-ClPhCO}_2)_4(THF)_2]$ and $[Ru_2(2\text{-MeO-4-ClPhCO}_2)_4(THF)_2]$ (Ru : Rh = 29 : 1, 19 : 1, or 8 : 2) was used instead of $[Ru_2(2\text{-MeO-4-ClPhCO}_2)_4(THF)_2]$. For **Rh-3%**, elemental analysis (%); calcd for $[(Ru_2)_{0.97}(Rh_2)_{0.03}(2\text{-MeO-4-ClPhCO}_2)_4(BTDA\text{-}TCNQ)]\cdot2.4(benzene)$ $C_{58.4}H_{38.4}Cl_4N_8O_{12}Rh_{0.06}Ru_{1.94}S_2$: C, 48.30; H, 2.66; N, 7.72. Found: C, 47.94; H, 2.76; N, 7.25. FT-IR (KBr): $\nu(C\equiv N)$, 2190, 2170; $\nu(C=O)$, 1596, 1405, 1381. For **Rh-5%**, elemental analysis (%); calcd for $[(Ru_2)_{0.95}(Rh_2)_{0.05}(2\text{-MeO-4-ClPhCO}_2)_4(BTDA\text{-}TCNQ)]\cdot2.5(benzene)$ $C_{59}H_{39}Cl_4N_8O_{12}Rh_{0.1}Ru_{1.9}S_2$: C, 48.53; H, 2.69; N, 7.67. Found: C, 48.40; H, 2.74; N, 7.22. FT-IR (KBr): $\nu(C\equiv N)$, 2190, 2167; $\nu(C=O)$, 1596, 1405, 1381. For **Rh-16%**, elemental analysis (%); calcd for $[(Ru_2)_{0.84}(Rh_2)_{0.16}(2\text{-MeO-4-ClPhCO}_2)_4(BTDA\text{-}TCNQ)]\cdot2.5(benzene)$ $C_{59}H_{39}Cl_4N_8O_{12}Rh_{0.32}Ru_{1.68}S_2$: C, 48.51; H, 2.69; N, 7.67. Found: C, 48.17; H, 2.69; N, 7.19. FT-IR (KBr): $\nu(C\equiv N)$, 2190, 2168; $\nu(C=O)$, 1595, 1406, 1380.

Identification and physical measurements.

Infrared spectra were measured using a KBr disk with a HORIBA FT-720 spectrophotometer. The X-ray fluorescent spectroscopy to analyze the existence of Ru and Rh elements in a single crystal was performed at room temperature with a continuous X-ray from a Cu source without graphite monochromator using Rigaku R-AXIS RAPID II with an ELement ANalyzer attachment. The single crystal was mounted on a MicroLoops LD (ϕ = 100 μm), and before the measurements, the diffraction pattern was checked at room temperature to confirm the crystallinity of samples. The presence of Ru and Rh atom was identified using $K\alpha$ and $K\beta_1$ lines of each metal. DC electrical resistivity on a single crystal was measured at a cryostat by a two-probe method with a KEITHLEY 2182A nanovoltmeter. Electrical contacts to the crystal were made with 3 μm diameter platinum wires and carbon pastes, and the source voltage was fixed at 0.1 V for the temperature-variable measurements, where the axis arrangement with a chain running direction in the crystal used was confirmed by the single-crystal X-ray crystallography before measuring. Temperature-dependent ac impedance was measured using a two-probe ac impedance method at frequencies in the range of 100 Hz–1 MHz (Hewlett-Packard HP4194A). A single crystal was placed into a cryogenic refrigeration system (Sumitomo Heavy Industories SRDK-101D). The electrical contacts were prepared using gold paste (Tokuriki 8560) to attach the 10 μm diameter gold wires to the single crystal. Magnetic susceptibility measurements were performed using a Quantum Design SQUID magnetometer (MPMS-XL). Dc measurements were conducted over the temperature range 1.8–300 K and from –7 T to +7 T. Ac measurements were performed at a frequency of 1 Hz with an ac field amplitude of 3 Oe and in the absence of a dc field. The measurements were performed on finely ground polycrystalline samples restrained by Nujol. Diamagnetic contributions were corrected for the sample holder, Nujol, and for the sample using Pascal's constants.[3]

ICP-MS. The Ru : Rh molar ratio of the Rh-doped samples was determined by inductively coupled plasma mass spectroscopy (ICP-MS). Analytical standards were purchased from Perkin Elmer Inc. All dilutions were done using a 3% HCl solution. All samples were analyzed for [102]Ru and [103]Rh simultaneously using SPQ9000 (SII NanoTechnology Inc.). About 1 mg of sample was weighed and dissolved in a concentrated HNO_3/H_2O_2 1:1 solution (2 ml) by heating at 100 °C, and then H_2O_2 was boiled off. The resulting solution was diluted to 100 ml, and a 1 ml portion was diluted to a 100 ml portion. The Ru : Rh ratio of each sample was measured using a calibration curve of aqueous standard at 0.2, 0.5, 1, 5, 10, 20 ppb for each metal.

X-ray Crystallography for 1, Rh-3%, Rh-5%, Rh-16%, and 1-Rh.

Single crystals of **1**, **Rh-3%**, **Rh-5%**, **Rh-16%**, and **1-Rh** were prepared according to the method described in the synthetic procedure. The single crystal was mounted on a thin kapton film with

Nujol and was cooled to 97±1 K by a stream of cooled N_2 gas. Data collections were made on a Rigaku CCD diffractometer (Mercury70+varimax) with graphite-monochromated MoKα radiation (λ = 0.71070 Å). The full-matrix least-squares refinement on F^2 was performed based on observed reflections and variable parameters and the refinement cycle was estimated from unweighted and weighted agreement factors of $R_1 = \Sigma||F_o|-|F_c||/\Sigma|F_o|$ ($I > 2.00\sigma(I)$ and all data), and $wR_2 = [\Sigma(w(F_o^2-F_c^2)^2)/\Sigma w(F_o^2)^2]^{1/2}$ (all data). A Sheldrick weighting scheme was used. Neutral atom scattering factors were taken from Cromer and Waber.[4] Anomalous dispersion effects were included in F_{calcd};[5] the values of $\Delta f'$ and $\Delta f''$ were those of Creagh and McAuley.[6] The values for the mass attenuation coefficients are those of Creagh and Hubbell.[7] All calculations were performed using the CrystalStructure crystallographic software package[8] except for refinement, which was performed using SHELXL-97.[9] Crystallographic data for **1**, **Rh-3%**, **Rh-5%**, **Rh-16%**, and **1-Rh** were summarized in Table S1. The CIF data for **1**, **Rh-3%**, **Rh-5%**, **Rh-16%**, and **1-Rh** have been deposited at the Cambridge Data Centre as supplementary publication No. CCDC-895011, 967287, 967288, 967286, and 895009, respectively. Copies of the data can be obtained free of charge on application to CCDC, 12 Union Road, Cambridge CB21EZ, UK (fax: (+44) 1223-336-033; email: deposit@ccdc.cam.ac.uk).

Computational Details.

Theoretical ab initio calculations of $[Ru_2^{II,II}(2\text{-MeO-4-ClPhCO}_2)_4(\text{THF})_2]$ and BTDA-TCNQ were performed using the density functional theory (DFT) formalism, as implemented in the Gaussian 09 software,[10] with the Beck's three parameter hybrid functional with the correlation functional of Lee, Yang and Parr (B3LYP).[11] Unrestricted open-shell calculations were performed in the calculations of the molecule containing $[Ru_2]$ units. An effective core potential basis set LanL2TZ with polarization (LanL2TZ(f))[12] for Ru, Pt and Pd atoms and 6-31G basis sets with polarization and diffuse functions (6-31+G(d))[13] for C, H, Cl, N, O and S atoms were adopted. In the calculations, spin polarization with $S_Z = 1$ (triplet spin multiplicity) for $[Ru_2]$ units was used. The atomic coordinates for determined by using X-ray crystallography were used in the calculation of $[Ru_2^{II,II}(2\text{-MeO-4-ClPhCO}_2)_4(\text{THF})_2]$.

Details of Crystal Structure of 1

There are two kinds of [Ru$_2$] moieties in the asymmetric unit, albeit very similar to each other, each of which has an inversion center at the midpoint of Ru–Ru bond, so the repeating unit can be described as a half of [–{Ru(1)$_2$}–(BTDA-TCNQ)–{Ru(2)$_2$}–(BTDA-TCNQ)–]. The Ru–O$_{eq}$ length (O$_{eq}$ = equatorial oxygen atoms) is quite sensitive to the oxidation state of the [Ru$_2$] unit: 2.06 – 2.07 Å for [Ru$_2^{II,II}$] and 2.02 – 2.03 Å for [Ru$_2^{II,III}$]$^+$.[14,15] The average Ru–O$_{eq}$ length is 2.016 Å for both [Ru$_2$] units (Table S2), indicating the oxidation state of [Ru$_2^{II,III}$]$^+$. While, the charge on the BTDA-TCNQ moiety was roughly estimated as $\rho = -1.32$ by using the Kistenmacher relationship of $\rho = A_\rho[c/(b + d)] + B_\rho$[16] in relation to a neutral species BTDA-TCNQ^0 ($\rho = 0$)[17] and an ionic species (NEtMe$_3$)(BTDA-TCNQ) ($\rho = -1$)[18] with $A_\rho = -50.00$ and $B_\rho = 23.25$, where b, c, and d are bond lengths of component bonds defined in Table S3.

Table S1. Crystallographic Data for **1, Rh-3%, Rh-5%, Rh-16%,** and **1-Rh.**

	1	Rh-3%	Rh-5%	Rh-16%	1-Rh
formula	$C_{59}H_{39}Cl_4N_8O_{12}Ru_2S_2$	$C_{59}H_{39}Cl_4N_8O_{12}Rh_{0.06}Ru_{1.94}S_2$	$C_{59}H_{39}Cl_4N_8O_{12}Rh_{0.1}Ru_{1.9}S_2$	$C_{59}H_{39}Cl_4N_8O_{12}Rh_{0.32}Ru_{1.68}S_2$	$C_{57.5}H_{37.5}Cl_4N_8O_{12}Rh_2S_2$
formula weight	1460.08	1460.19	1460.26	1460.66	1444.22
crystal system	triclinic	triclinic	triclinic	triclinic	triclinic
space group	P-1 (#2)	P-1 (#2)	P-1 (#2)	P-1 (#2)	P-1 (#2)
a / Å	10.479(2)	10.4829(12)	10.4807(13)	10.4709(12)	10.407(2)
b / Å	16.567(3)	16.544(2)	16.548(2)	16.556(2)	16.616(3)
c / Å	17.166(3)	17.220(2)	17.218(2)	17.224(2)	17.220(3)
α / deg	84.697(4)	84.962(4)	84.951(4)	84.981(4)	85.105(6)
β / deg	89.874(4)	89.741(4)	89.769(4)	89.787(4)	89.676(5)
γ / deg	80.039(3)	80.141(4)	80.148(3)	80.170(3)	80.244(5)
V / Å^3	2922.4(8)	2930.9(6)	2930.6(6)	2932.2(6)	2923.8(8)
Z	2	2	2	2	2
crystal size	$0.11 \times 0.06 \times 0.05$	$0.233 \times 0.140 \times 0.052$	$0.196 \times 0.145 \times 0.048$	$0.166 \times 0.159 \times 0.022$	$0.186 \times 0.092 \times 0.012$
T / K	97	97	97	97	97
D_{calc} / g cm^{-3}	1.659	1.654	1.655	1.654	1.640
F_{000}	1466	1466.12	1466.20	1466.64	1449
λ / Å	0.71075	0.71075	0.71075	0.71075	0.71075
μ(Mo Kα) / cm^{-1}	8.420	8.409	8.419	8.466	8.868
data mesured	19560	19987	19941	19944	20051
data unique	10011	10103	10106	10103	10071
R_{int}	0.0169	0.0200	0.0221	0.0277	0.0484
No. of obs. (All reflections)	10011	10103	10106	10103	10071
No. of variables	784	784	784	784	793
$R1$ ($I > 2.00s(I)$)[a]	0.0373	0.0471	0.0485	0.0481	0.0608
R (all refrections)[a]	0.0476	0.0547	0.0562	0.0566	0.0883
$wR2$ (all refrections)[b]	0.0992	0.1357	0.1374	0.1388	0.1672
GOF	1.052	1.062	1.049	1.048	1.061
CCDC no.	895011	967287	967288	967286	895009

[a]$R1 = \Sigma||F_o| - |F_c|| / \Sigma|F_o|$. [b]$wR2 = [\Sigma w(F_o^2 - F_c^2)^2 / \Sigma w(F_o^2)^2]^{1/2}$.

Table S2. Relevant Bond Lengths around Metal Centers, where M = Ru or Rh, N_{ax} = N Atom of BTDA-TCNQ, and O_{eq} = Carboxylate Oxygen Atoms

Compound	Asymmetric [M_2] unit	M–M / Å	M–N_{ax} / Å	M–O_{eq} / Å				
				M–O_{eq}(1)	M–O_{eq}(2)	M–O_{eq}(3)	M–O_{eq}(4)	Ave. M–O_{eq}
1	Ru(1)	2.2827(4)	2.252(3)	2.023(5)	2.016(2)	2.006(2)	2.018(2)	2.016
	Ru(2)	2.2823(4)	2.247(3)	2.015(2)	2.017(2)	2.016(2)	2.014(2)	2.016
Rh-3%	M(1)	2.2864(4)	2.253(4)	2.015(3)	2.017(3)	2.017(3)	2.021(3)	2.018
	M(2)	2.2862(5)	2.253(4)	2.007(3)	2.016(3)	2.011(3)	2.029(3)	2.016
Rh-5%	M(1)	2.2877(5)	2.250(4)	2.014(3)	2.016(3)	2.019(3)	2.022(3)	2.018
	M(2)	2.2879(5)	2.248(4)	2.008(3)	2.018(3)	2.029(3)	2.011(3)	2.017
Rh-16%	M(1)	2.2999(5)	2.244(4)	2.017(3)	2.018(3)	2.022(3)	2.022(3)	2.020
	M(2)	2.3006(5)	2.248(4)	2.012(3)	2.023(3)	2.026(3)	2.014(3)	2.019
1-Rh	Rh(1)	2.3892(7)	2.209(5)	2.045(5)	2.026(5)	2.023(4)	2.042(4)	2.034
	Rh(2)	2.3863(6)	2.212(5)	2.030(4)	2.027(4)	2.035(5)	2.020(4)	2.028

Table S3. **Comparison of Bond Distances (Å) in the BTDA-TCNQ Moiety of 1, Rh-3%, Rh-5%, Rh-16%, and 1-Rh**
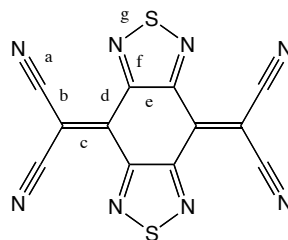
Compound	a	b	c	d	e	f	g	ρ_c [c]	$\rho_{c/d}$ [d]	$\rho_{c/(b+d)}$ [e]
I [f]	1.126(5)	1.444(6)	1.351(7)	1.464(6)	1.421(5)	1.330(5)	1.626(4)	0	0	0
II [g]	1.140(6)	1.429(7)	1.390(6)	1.437(6)	1.433(5)	1.346(6)	1.614(4)	−1	−1	−1
1	1.144(5)	1.428(6)	1.406(5)	1.434(5)	1.445(5)	1.336(4)	1.614(3)			
	1.156(5)	1.428(5)	1.402(4)	1.436(4)	1.445(5)	1.349(4)	1.610(3)			
	1.139(4)	1.425(5)		1.436(5)		1.340(4)	1.608(3)			
	1.157(5)	1.421(4)		1.433(5)		1.352(4)	1.608(3)			
	1.149 [a]	1.426 [a]	1.404 [a]	1.435 [a]	1.445 [a]	1.344 [a]	1.610 [a]	−1.36 [b]	−1.26 [b]	−1.29 [b]
Rh-3%	1.132(5)	1.426(6)	1.403(6)	1.430(5)	1.443(6)	1.347(5)	1.611(4)			
	1.152(6)	1.431(6)	1.399(6)	1.439(6)	1.438(6)	1.342(6)	1.611(4)			
	1.142(6)	1.430(6)		1.442(5)		1.346(5)	1.617(4)			
	1.161(6)	1.420(6)		1.442(6)		1.338(5)	1.612(4)			
	1.147 [a]	1.427 [a]	1.401 [a]	1.438 [a]	1.441 [a]	1.343 [a]	1.613 [a]	−1.28 [b]	−1.17 [b]	−1.20 [b]
Rh-5%	1.132(6)	1.426(6)	1.401(6)	1.444(6)	1.447(6)	1.344(5)	1.608(4)			
	1.156(6)	1.429(6)	1.397(6)	1.441(6)	1.442(6)	1.347(6)	1.613(4)			
	1.146(6)	1.433(7)		1.444(6)		1.344(5)	1.612(4)			
	1.151(6)	1.423(6)		1.434(5)		1.339(6)	1.612(4)			
	1.146 [a]	1.428 [a]	1.399 [a]	1.441 [a]	1.445 [a]	1.344 [a]	1.611 [a]	−1.23 [b]	−1.09 [b]	−1.13 [b]
Rh-16%	1.135(6)	1.428(6)	1.396(6)	1.444(6)	1.437(6)	1.347(5)	1.611(4)			
	1.155(6)	1.427(6)	1.396(6)	1.440(6)	1.436(6)	1.344(6)	1.614(4)			
	1.137(6)	1.433(7)		1.443(6)		1.351(5)	1.613(4)			
	1.156(6)	1.425(6)		1.437(5)		1.337(6)	1.613(4)			
	1.146 [a]	1.428 [a]	1.396 [a]	1.441 [a]	1.437 [a]	1.345 [a]	1.613 [a]	−1.15 [b]	−1.04 [b]	−1.08 [b]
1-Rh	1.134(8)	1.431(9)	1.369(9)	1.461(9)	1.433(9)	1.315(8)	1.623(6)			
	1.147(8)	1.426(8)	1.376(8)	1.459(8)	1.430(9)	1.327(8)	1.622(5)			
	1.123(8)	1.430(9)		1.467(9)		1.314(8)	1.622(6)			
	1.143(8)	1.440(8)		1.459(8)		1.348(8)	1.607(5)			
	1.137 [a]	1.432 [a]	1.373 [a]	1.462 [a]	1.432 [a]	1.326 [a]	1.629 [a]	−0.56 [b]	−0.37 [b]	−0.47 [b]

[a] average value. [b] Estimated from the average values. [c] $\rho_c = A_1c + B_1$ with $A_1 = -25.64$ and $B_1 = 34.64$. [d] $\rho_{c/d} = A_2(c/d) + B_2$ with $A_2 = -22.73$ and $B_2 = 20.98$. [e] $\rho_{c/(b+d)} = A_3(c/(b+d)) + B_3$ with $A_3 = -50.00$ and $B_3 = 23.25$. [f] BTDA-TCNQ; Ref.17. [g] [NEt(Me)$_3$](BTDA-TCNQ); Ref.18.
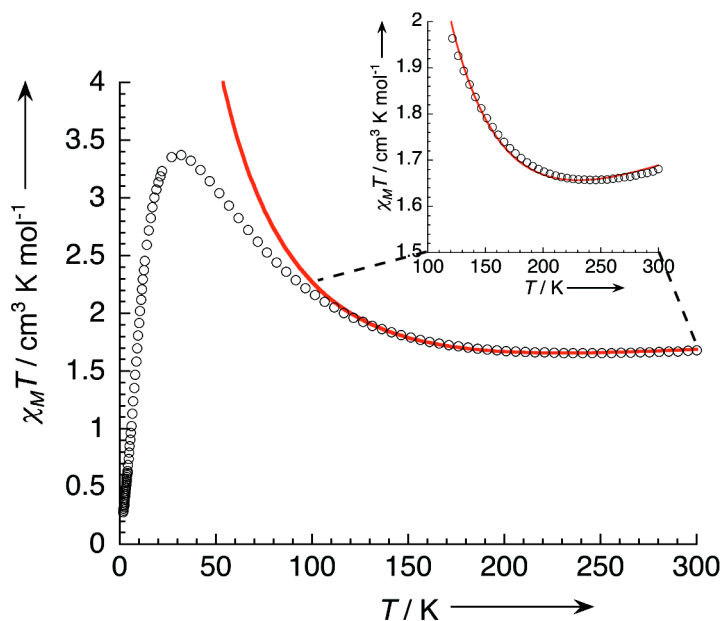
Figure S1. Temperature dependence of χT for **1** measured applying a dc field of 1 kOe, where the insets are close-up views for the range of 100–300 K. The data were simulated in the range of 120 – 300 K using an alternating chain model with S_i = 3/2 and S_{i+1} = ½ in the Hamiltonian $H = -2J \sum_{i=1}^{N} \vec{S}_i \cdot \vec{S}_{i+1}$, and an adequate parameter set was obtained as g_{Ru} = 2.08, g_{Rad} = 2.0 (fix) and J/k_B = –100.5 K. The exchange between $[Ru_2^{II,III}]^+$ and BTDA-TCNQ$^{\bullet-}$ is strong antiferromagnetic. The details will be discussed elsewhere.
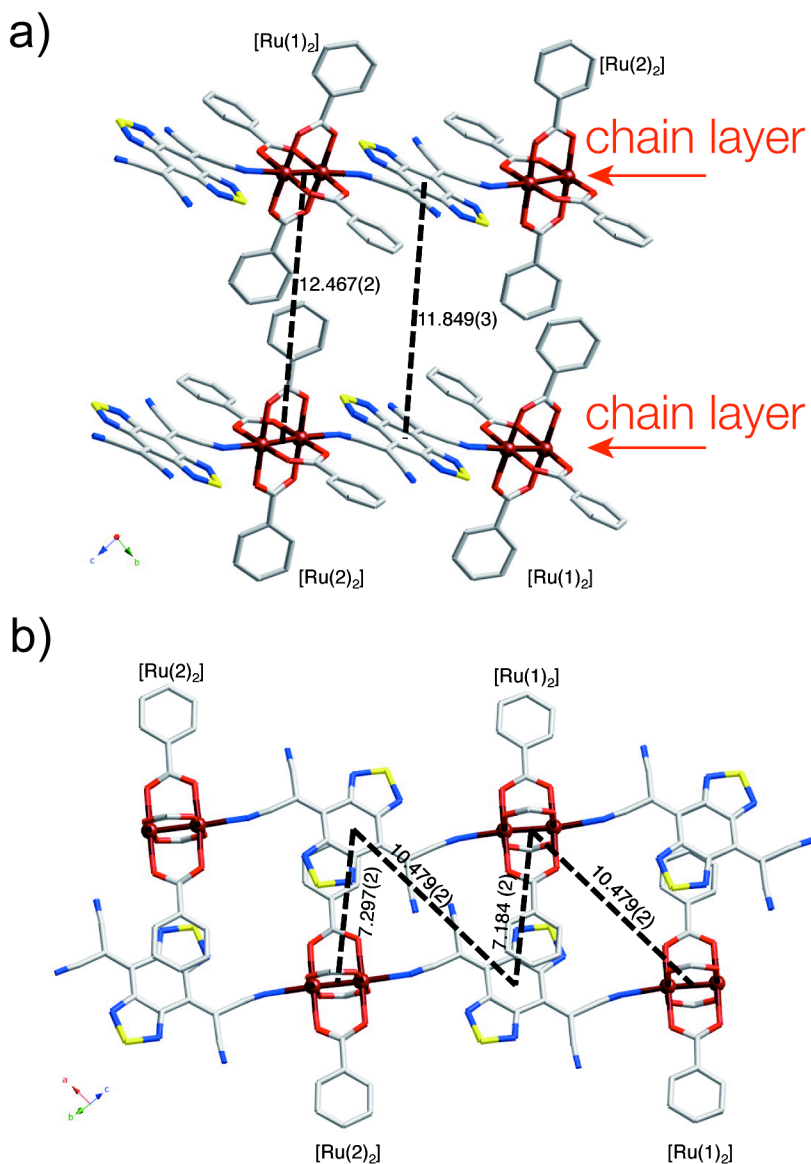
Figure S2. Packing diagrams with the definition of inter-chain distances for **1**, where Cl and methoxy groups and hydrogen atoms on phenyl rings were omitted for clarity and phenyl rings were omitted in part from (b) for clarity.
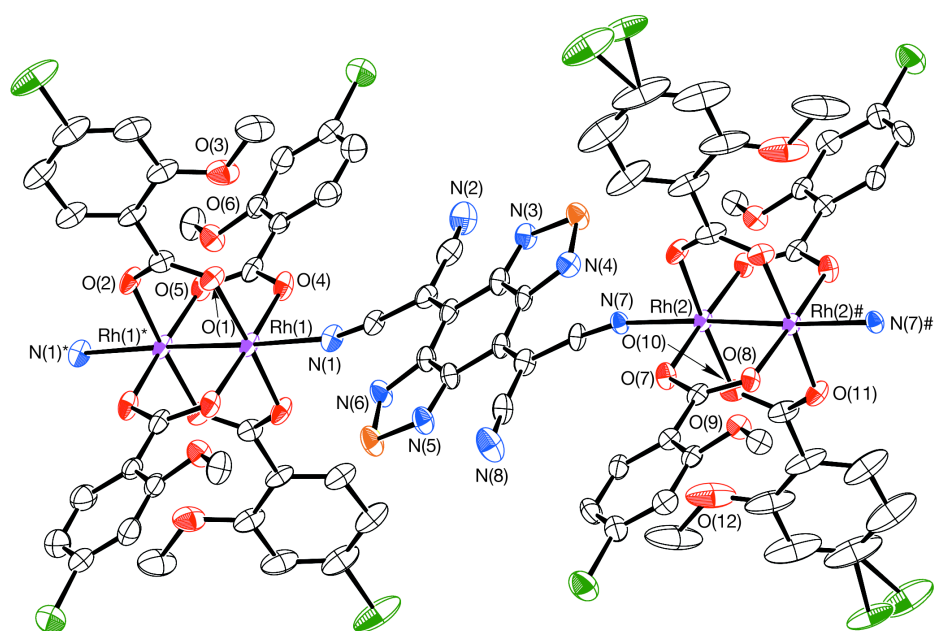
Figure S3. Structure of the asymmetric unit of **1-Rh** (50 % probability ellipsoids). Symmetry operation: * –*x*, –*y*+1, –*z*+2; # –*x*+2, –*y*+2, –*z*+1. Crystallographic data was summarized in Table S1.
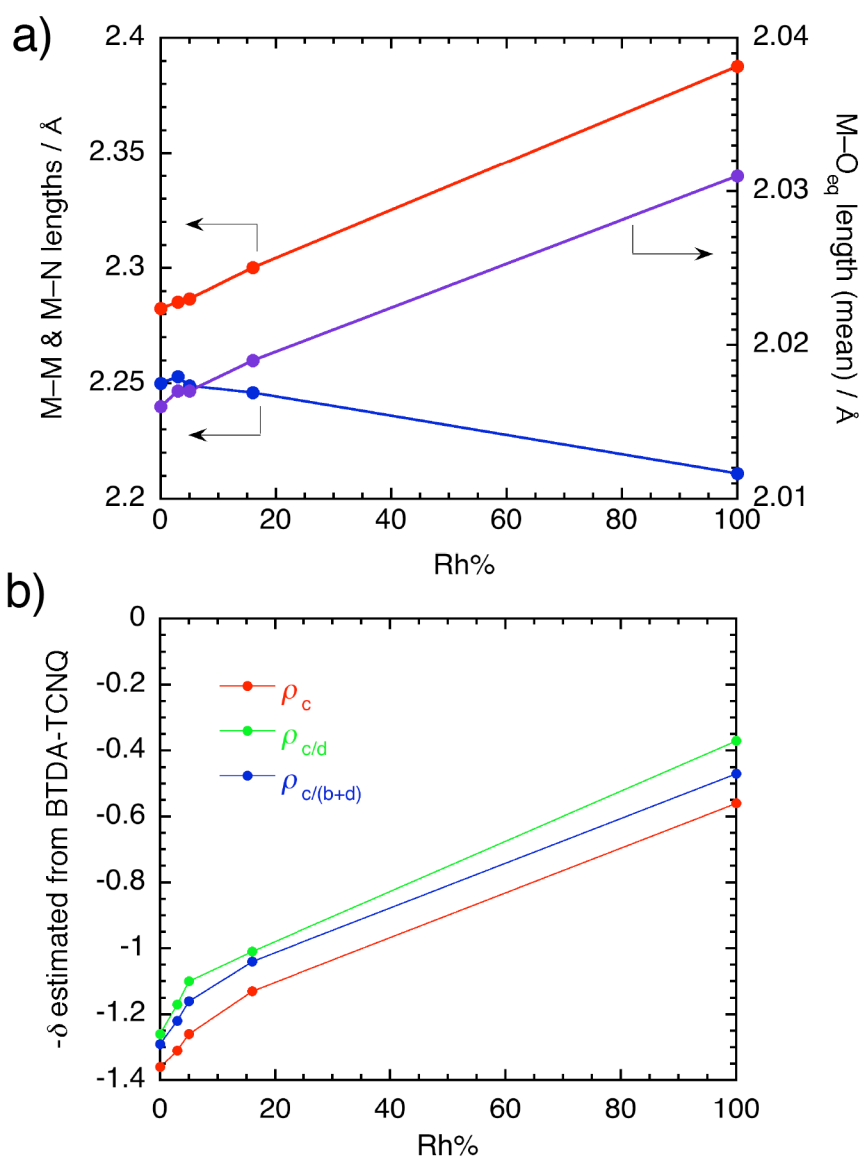
Figure S4. Structural comparison and valence (δ) of the BTDA-TCNQ moiety with the doping rate. (a) The M–M, M–N, and M–Oeq (mean) bond lengths. (b) δ value estimated from bond lengths in the BTDA-TCNQ moiety (see Table S3).
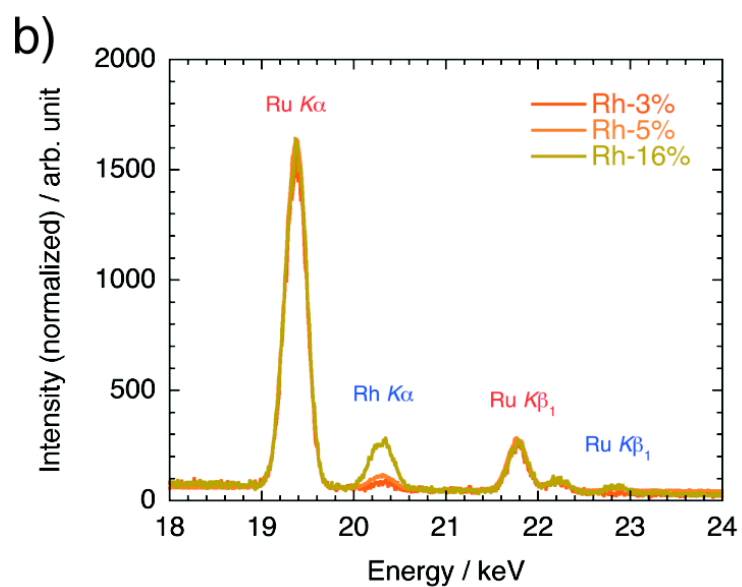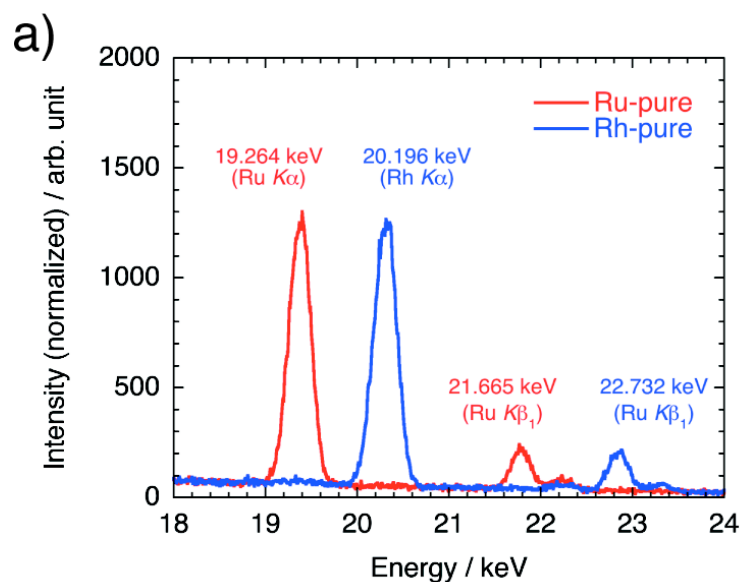
Figure S5. fluorescent X-ray spectra of **1** and **1-Rh** (a) and doped compounds (**Rh-3%**, **Rh-5%**, and **Rh-16%**) (b).
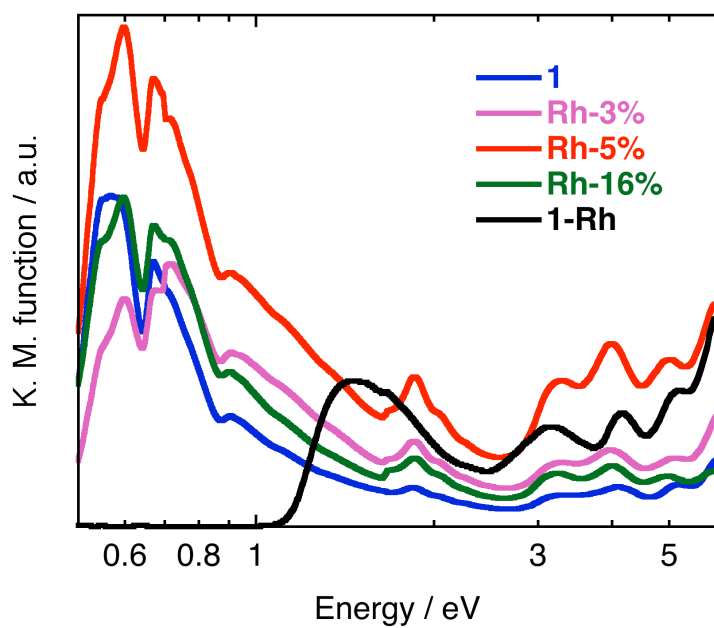
Figure S6. Powder reflection spectra of **1**, **Rh-3%**, **Rh-5%**, **Rh-16%**, and **1-Rh** measured using pellets diluted with $BaSO_4$.
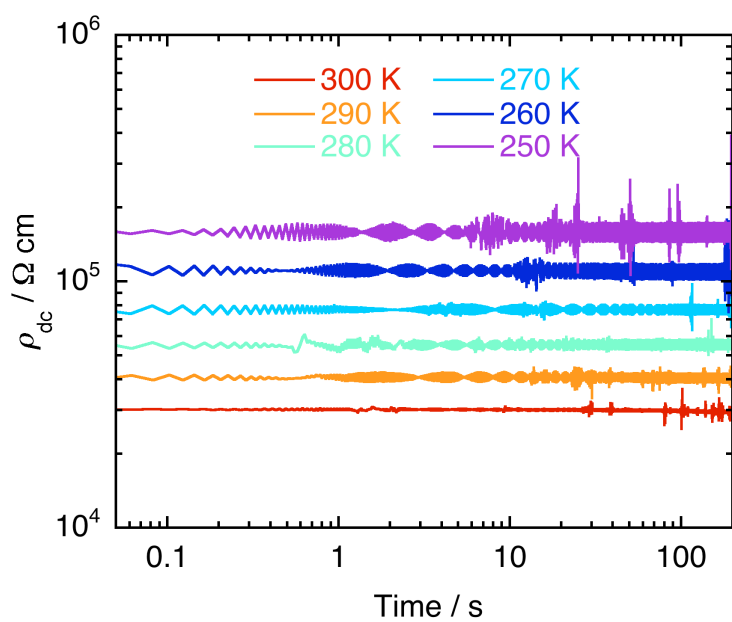
Figure S7. Time dependence of ρ_{dc} of **Rh-16%** measured at temperatures in the range of 250–300 K, where oscillating behavior is merely due to any noise come from the apparatus used.

References in SI

1   Miyasaka, H.; Motokawa, N.; Atsuumi, R.; Kamo, H.; Asai, Y.; Yamashita, M. *Dalton Trans.* **2011**, *40*, 673–682.

2   Drago, R. S.; Peter Tanner, S.; Richman, R. M.; Long, J. R. *J. Am. Chem. Soc.* **1979**, *101*, 2897–2903.

3   Boudreaux, E. A.; Mulay, L. N. *Theory and Applications of Molecular Paramagnetism*, Eds. John Wiley & Sons, New-York, **1976**.

4   Cromer, D. T.; Waber, J. T. *International Tables for Crystallography Vol IV*, The Kynoch Press, Birmingham, England, Table 2.2A, **1974**.

5   Ibers, J. A.; Hamilton, W. C. *Acta Crystallogr.* **1964**, *17*, 781.

6   Creagh, D. C.; McAuley, W. J. *International Tables for Crystallography Vol C*, (Wilson, A. J. C., Ed.), Kluwer Academic Publishers, Boston, Table 4.2.6.8, pp 219-222, **1992**.

7   Creagh, D. C.; Hubbell, J. H.; *International Tables for Crystallography Vol C*, (Wilson, A. J. C. Ed.), Kluwer Academic Publishers, Boston, Table 4.2.4.3, pp 200-206, **1992**.

8   CrystalStructure 4.0.1: Crystal Structure Analysis Package, Rigaku Corporation (2000-2010). Tokyo 196-8666, Japan.

9   SHELX97: Sheldrick, G. M. *Acta Cryst.* **2008**, *A64*, 112-122.

10 Gaussian 09, Revision B.01, Frisch, M. J.; Trucks, G. W.; Schlegel, H. B.; Scuseria, G. E.; Robb, M. A.; Cheeseman, J. R.; Scalmani, G.; Barone, V.; Mennucci, B.; Petersson, G. A.; Nakatsuji, H.; Caricato, M.; Li, X.; Hratchian, H. P.; Izmaylov, A. F.; Bloino, J.; Zheng, G.; Sonnenberg, J. L.; Hada, M.; Ehara, M.; Toyota, K.; Fukuda, R.; Hasegawa, J.; Ishida, M.; Nakajima, T.; Honda, Y.; Kitao, O.; Nakai, H.; Vreven, T.; Montgomery, Jr., J. A.; Peralta, J. E.; Ogliaro, F.; Bearpark, M.; Heyd, J. J.; Brothers, E.; Kudin, K. N.; Staroverov, V. N.; Kobayashi, R.; Normand, J.; Raghavachari, K.; Rendell, A.; Burant, J. C.; Iyengar, S. S.; Tomasi, J.; Cossi, M.; Rega, N.; Millam, J. M.; Klene, M.; Knox, J. E.; Cross, J. B.; Bakken, V.; Adamo, C.; Jaramillo, J.; Gomperts, R.; Stratmann, R. E.; Yazyev, O.; Austin, A. J.; Cammi, R.; Pomelli, C.; Ochterski, J. W.; Martin, R. L.; Morokuma, K.; Zakrzewski, V. G.; Voth, G. A.; Salvador, P.; Dannenberg, J. J.; Dapprich, S.; Daniels, A. D.; Farkas, Ö.; Foresman, J. B.; Ortiz, J. V.; Cioslowski, J.; Fox, D. J. Gaussian, Inc., Wallingford CT, 2009.

11 Becke, A. D. *J. Chem. Phys.*, **1993**, *98*, 5648.

12 (a) Hay, P. J. ; Wadt, W. R. *J. Chem. Phys.*, **1985**, *82*, 299. (b) Roy, L. E.; Hay, P. J.; Martin, R. L. *J. Chem. Theory Comput.*, **2008**, *4*, 1029. (c) Ehlers, A. W.; Böhme, M.; Dapprich, S.; Gobbi, A.; Höllwarth, A.; Jonas, V.; Köhler, K. F.; Stegmann, R.; Veldkamp, A.; Frenking, G. *Chem. Phys. Lett.*, **1993**, *208*, 111.

13 (a) Hariharan, P. C.; Pople, J. A. *Theoret. Chimica Acta*, **1973**, *28*, 213. (b) Francl, M. M.; Petro, W. J.; Hehre, W. J; Binkley, J. S.; Gordon, M. S.; DeFrees, D. J.; Pople, J. A. *J. Chem. Phys.*, **1982**, *77*, 3654. (c) Clark, T.; Chandrasekhar, J.; Schleyer, P. V. R. *J. Comp. Chem.*, **1983**, *4*, 294. (d) Krishnam, R.; Binkley, J. S.; Seeger, R.; Pople, J. A. *J. Chem. Phys.*, **1980**, *72*, 650. (e) Gill, P. M. W.; Johnson, B. G.; Pople, J. A.; Frisch, M. J. *Chem. Phys. Lett.*, **1992**, *197*, 499.

14 Cotton, F. A.; Walton, R. A. *Multiple Bonds Between Metal Atoms*, 2nd ed., Oxford University Press, Oxford, **1993**.

15 Miyasaka, H.; Motokawa, N.; Chiyo, T.; Takemura, M.; Yamashita, M.; Sagayama, H. Arima, T.; *J. Am. Chem. Soc.* **2011**, *133*, 5338–5345.

16 Kistenmacher, T. J.; Emge, T. J.; Bloch, A. N. Cowan, D. O.; *Acta Crystallogr., Sect. B* **1982**,

  38, 1193–1199.

17 Suzuki, T.; Fujii, H.; Yamashita, Y.; Kabuto, C.; Tanaka, S.; Harasawa, M.; Mukai, T.; Miyashi, T. *J. Am. Chem. Soc.* **1992**, *114*, 3034–3043.

18 Suzuki, T.; Kabuto, C.; Yamashita, Y.; Mukai, T.; Miyashi, T.; Saito, G. *Bull. Chem. Soc. Jpn.* **1988**, *61*, 483–493.